Transition radiation at the boundary of a chiral isotropic medium

Sergey N. Galyamin* and Andrey V. Tyukhtin†
Saint Petersburg State University, 7/9 Universitetskaya nab., St. Petersburg 199034, Russia

Anton A. Peshkov
Saint Petersburg State University, 7/9 Universitetskaya nab., St. Petersburg 199034, Russia
and Helmholtz-Institut Jena, Fröbelstieg 3, Jena 07743, Germany

(Received 14 November 2016; revised manuscript received 11 January 2017; published 29 March 2017)

This study analyzes the radiation produced by a point charge intersecting the interface between a vacuum and a chiral isotropic medium. We deduce analytical expressions for the Fourier components of an electromagnetic field in both vacuum and medium for arbitrary charge velocity. The main focus is on investigating the far field in a vacuum. The distinguishing feature of the interface with a chiral isotropic medium is that the field in the vacuum area contains both copolarization (coinciding with the polarization of the self-field of a charge) and cross-polarization (orthogonal to the polarization of the self-field). Using a saddle-point approach, we obtain asymptotic representations for the field components in the far-field zone for typical frequency ranges of the Condon model of the chiral medium. We note that a so-called lateral wave is generated in a vacuum for certain parameters. The main contribution to the radiation at large distances is presented by two (co- and cross-) spherical waves of transition radiation. These waves are coherent and result in a total spherical wave with elliptical polarization, with the polarization coefficient being determined by the chirality of the medium. We present typical radiation patterns and ellipses of polarization.

DOI: 10.1103/PhysRevE.95.032142

I. INTRODUCTION

Research in the field of optical activity (or chirality, or gyrotropy) has a long history since the discovery of so-called optical rotatory power [1]. The studies have involved investigations of various aspects of electrodynamics of chiral media collected in a series of reviews and books [2–6]. It should be noted that most biological tissues are chiral isotropic media because they possess chirality due to the mirrorless structure of molecules [7–9].

The science of radiation from charged particles uniformly moving in material media, which is connected with the experimental discovery [10] and corresponding theoretical explanation [11] of Cherenkov radiation, is approximately 80 years old [12–14]. During this period, some aspects of Cherenkov radiation in various chiral media have been investigated in several papers [15–20]. In particular, a detailed investigation of the structure of the electromagnetic field produced by a point charge uniformly moving in a chiral isotropic medium obeying the Condon model of frequency dispersion [4] was performed in our previous paper [21]. In paper [21], the reader can also found references to numerous papers on field potentials and Green's functions in chiral media, a "dictionary" on constitutive relations, and papers dealing with chiral interfaces, guided waves, and electromagnetic properties of distinct chiral objects (recent investigation of modern chiral nanostructures can be found in Ref. [22]). A similar problem with a chiral anisotropic medium was considered in Ref. [23]. Another related effect, transition radiation [24], for the case of interface with a chiral medium was partially analyzed in the limiting case of slow charge motion [25].

However, in recent years, renewed interest in the aforementioned effects has emerged due to the development of a relatively new prospective method for the diagnostics of biological objects—Cherenkov luminescence tomography (CLT) [26–33]. This method is based on the registration of Cherenkov light emitted by electrons or protons, which are in turn produced during the radioactive decay of radionuclides placed in the tissue under investigation. For example, cancer diagnostics can be performed with CLT, if the radioactively labeled glucose molecules are injected into the investigated body. CLT can also be used for precise tracking of labeled antibodies in radioimmunotherapy. In contrast to other techniques such as positron emission tomography, where expensive γ-ray detectors are required, CLT utilizes visible light that can be registered using conventional light sensors [34]. The first experiments in human CLT have been reported recently [35].

In this paper, we investigate the effect of the simplest inhomogeneity (a planar interface) on radiation produced by a moving charge in chiral medium. We consider the typical formulation of the transition radiation problem in which a uniformly moving point charge orthogonally intersects the plane boundary between a vacuum and a chiral isotropic medium. On the one hand, we continue the investigation of our previous paper [21]; on the other hand, we perform a generalization of an earlier paper [25], since we suppose that the charge motion velocity is arbitrary.

The paper is organized as follows. After the introduction (Sec. I), we briefly discuss properties of the electromagnetic field in an unbounded chiral medium (Sec. II). Section III contains a rigorous solution for the field of transition radiation and several limiting cases. Section IV is devoted to the asymptotic investigation of the radiation in the far-field zone of the vacuum area. In Sec. V, the specific frequency dispersion (Condon model) is utilized for the graphical representation

*s.galyamin@spbu.ru
†a.tyuhtin@spbu.ru

of typical radiation patterns and ellipses of polarization. The conclusion (Sec. VI) finishes the paper.

II. MATERIAL RELATIONS AND FIELD POTENTIALS FOR CHIRAL ISOTROPIC MEDIUM

In this paper, we will describe the isotropic chiral media by the following symmetrized material relations [21,36]:

$$\begin{aligned}\vec{D}_\omega &= \varepsilon(\omega)\vec{E}_\omega - i\varkappa(\omega)\vec{H}_\omega,\\ \vec{B}_\omega &= \mu(\omega)\vec{H}_\omega + i\varkappa(\omega)\vec{E}_\omega.\end{aligned} \tag{1}$$

Here, $\varkappa$ is a chiral parameter, ε and μ are the dielectric permittivity and magnetic permeability, respectively, and values with the subscript ω are the time Fourier transforms of electromagnetic field components:

$$\{\vec{E}_\omega, \vec{D}_\omega, \vec{H}_\omega, \vec{B}_\omega\} = \frac{1}{2\pi}\int_{\mathbb{R}} \{\vec{E}, \vec{D}, \vec{H}, \vec{B}\}e^{i\omega t}dt. \tag{2}$$

As usual, because the field components are real values,

$$\begin{aligned}&\{\vec{E}_\omega(-\bar{\omega}), \vec{D}_\omega(-\bar{\omega}), \vec{H}_\omega(-\bar{\omega}), \vec{B}_\omega(-\bar{\omega})\}\\ &\quad= \{\overline{\vec{E}_\omega}(\omega), \overline{\vec{D}_\omega}(\omega), \overline{\vec{H}_\omega}(\omega), \overline{\vec{B}_\omega}(\omega)\},\end{aligned} \tag{3}$$

where the overline indicates a complex conjugate. The inverse Fourier transform

$$\{\vec{E}, \vec{D}, \vec{H}, \vec{B}\} = \int_{\mathbb{R}} \{\vec{E}_\omega, \vec{D}_\omega, \vec{H}_\omega, \vec{B}_\omega\}e^{-i\omega t}d\omega \tag{4}$$

can be rewritten in accordance with Eq. (3) in the following form:

$$\{\vec{E}, \vec{D}, \vec{H}, \vec{B}\} = 2\,\mathrm{Re}\int_0^\infty \{\vec{E}_\omega, \vec{D}_\omega, \vec{H}_\omega, \vec{B}_\omega\}e^{-i\omega t}d\omega. \tag{5}$$

Using Eq. (1), we can write the Maxwell equations for time Fourier transforms in the form

$$\begin{aligned}\mathrm{rot}\,\vec{E}_\omega &= \frac{i\omega}{c}[\mu\vec{H}_\omega + i\varkappa\,\vec{E}_\omega],\\ \mathrm{rot}\,\vec{H}_\omega &= \frac{-i\omega}{c}[\varepsilon\vec{E}_\omega - i\varkappa\,\vec{H}_\omega] + \frac{4\pi}{c}\vec{j}_\omega,\end{aligned} \tag{6}$$

$$\mathrm{div}\,\vec{E}_\omega = \frac{4\pi\mu}{\varepsilon\mu - \varkappa^2}\rho_\omega, \quad \mathrm{div}\,\vec{H}_\omega = -\frac{4\pi i\varkappa}{\varepsilon\mu - \varkappa^2}\rho_\omega, \tag{7}$$

where ρ_ω and $\vec{j}_\omega$ are the time Fourier transforms of the charge and current densities of the sources, respectively. After a series of transformations, by introducing the new unknown vectors $\vec{E}^+_\omega$ and $\vec{E}^-_\omega$ (to play the role of potentials) [3,19,21],

$$\begin{aligned}\vec{E}_\omega &= \vec{E}^+_\omega + \vec{E}^-_\omega,\\ \vec{H}_\omega &= \vec{H}^+_\omega + \vec{H}^-_\omega = i\frac{\sqrt{\varepsilon\mu}}{\mu}(\vec{E}^+_\omega - \vec{E}^-_\omega),\end{aligned} \tag{8}$$

we obtain the following uncoupled equations [21]:

$$\begin{aligned}&\Delta\vec{E}^\pm_\omega + \frac{\omega^2}{c^2}n_\pm^2\vec{E}^\pm_\omega\\ &\quad= \frac{2\pi\mu}{\sqrt{\varepsilon\mu}}\left(-i\frac{\omega}{c^2}n_\pm\vec{j}_\omega + \frac{1}{n_\pm}\nabla\rho_\omega \pm \frac{i}{c}\mathrm{rot}\vec{j}_\omega\right),\end{aligned} \tag{9}$$

where

$$n_\pm = n \pm \varkappa, \quad n = \sqrt{\varepsilon\mu}. \tag{10}$$

It is convenient to determine the radical in (10) by the rule $\mathrm{Re}\sqrt{\varepsilon\mu} > 0$ for real positive or complex values of the product $\varepsilon\mu$ and by the rule $\sqrt{\varepsilon\mu} = i|\sqrt{\varepsilon\mu}|$ for real negative values of $\varepsilon\mu$ [21]. With these definitions, we have

$$n_\pm(-\bar{\omega}) = \overline{n_\mp(\omega)}. \tag{11}$$

Note that the particular solution of (9) for the case of a moving point charge in a homogeneous unbounded medium was obtained in Ref. [21]. For analysis that will be performed in Sec. III, some additional convenient expressions can be obtained from (9) (see Appendix A).

As follows from (9), two plane monochromatic waves can exist in the medium under consideration:

$$\vec{E}^+_\omega = \vec{E}^+_{\omega 0}\exp(i\vec{k}_+\vec{R}), \quad \vec{E}^-_\omega = \vec{E}^-_{\omega 0}\exp(i\vec{k}_-\vec{R}). \tag{12}$$

They have complex magnitudes

$$\vec{E}^\pm_{\omega 0} = \vec{E}'^\pm_{\omega 0} + i\vec{E}''^\pm_{\omega 0}, \quad \vec{H}^\pm_{\omega 0} = \vec{H}'^\pm_{\omega 0} + i\vec{H}''^\pm_{\omega 0}, \tag{13}$$

and wave vectors

$$\vec{k}_\pm = k_\pm\vec{e}_k, \quad k_\pm = k_0 n_\pm, \quad k_0 = \omega/c, \tag{14}$$

where $\vec{e}_k$ is a unit vector determining the direction of wave propagation. Combining (7) with $\rho_\omega = 0$, one can obtain that the following scalar multiplications equal zero,

$$(\vec{e}_k, \vec{E}'^\pm_{\omega 0}) = (\vec{e}_k, \vec{E}''^\pm_{\omega 0}) = (\vec{e}_k, \vec{H}'^\pm_{\omega 0}) = (\vec{e}_k, \vec{H}''^\pm_{\omega 0}) = 0, \tag{15}$$

and therefore the waves (12) are transversal. Combining (6) with $\vec{j}_\omega = 0$, one can obtain

$$[\vec{e}_k, \vec{E}'^\pm_{\omega 0}] = \mp\vec{E}''^\pm_{\omega 0}, \quad [\vec{e}_k, \vec{E}''^\pm_{\omega 0}] = \pm\vec{E}'^\pm_{\omega 0}, \tag{16}$$

$$[\vec{e}_k, \vec{H}'^\pm_{\omega 0}] = \mp\vec{H}''^\pm_{\omega 0}, \quad [\vec{e}_k, \vec{H}''^\pm_{\omega 0}] = \pm\vec{H}'^\pm_{\omega 0}, \tag{17}$$

where square brackets refer to vector multiplication. The combination of (6), (16), and (17) gives

$$\vec{H}'^\pm_{\omega 0} = \mp Z^{-1}\vec{E}''^\pm_{\omega 0}, \quad \vec{H}''^\pm_{\omega 0} = \pm Z^{-1}\vec{E}'^\pm_{\omega 0}, \tag{18}$$

where $Z = \mu/\sqrt{\varepsilon\mu}$. If we suppose that the Fourier spectrum contains a single frequency ω (harmonic regime) then $\vec{E}^\pm = \mathrm{Re}[\vec{E}^\pm_\omega\exp(-i\omega t)]$, and we obtain

$$\vec{E}^\pm = \vec{E}'^\pm_{\omega 0}\cos[k_\pm(\vec{e}_k, \vec{R}) - \omega t] - \vec{E}''^\pm_{\omega 0}\sin[k_\pm(\vec{e}_k, \vec{R}) - \omega t], \tag{19}$$

$$\begin{aligned}\vec{H}^\pm = \mp Z^{-1}\{&\vec{E}'^\pm_{\omega 0}\sin[k_\pm(\vec{e}_k, \vec{R}) - \omega t]\\ &+ \vec{E}''^\pm_{\omega 0}\cos[k_\pm(\vec{e}_k, \vec{R}) - \omega t]\}.\end{aligned} \tag{20}$$

Figure 1 illustrates formulas (19) and (20) for $Z < 1$ and $|\varkappa| < |n|$. For definiteness, we use a Cartesian frame x', y', z' and suppose that $\vec{e}_k = \vec{e}_{z'}$, and therefore $(\vec{e}_k, \vec{R}) = z'$, and waves propagate along the z' axis. If an observer is situated in plane $z' = 0$, and waves propagate to the observer, then vectors $\vec{E}^+$ and $\vec{H}^+$ rotate clockwise while vectors $\vec{E}^-$ and $\vec{H}^-$ rotate counterclockwise in the (x', y') plane. In other words, these waves possess circular polarization. We will further refer to the $+$ and $-$ waves as waves with right- and left-hand polarizations, respectively. Moreover, if we introduce

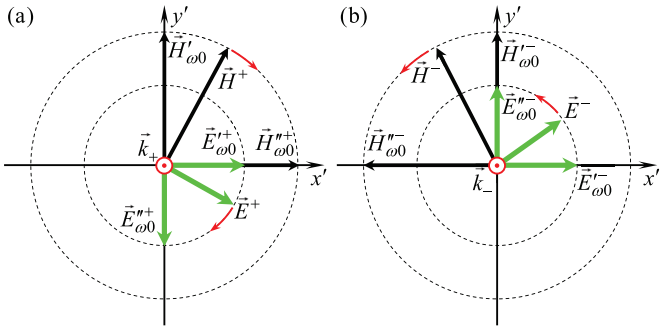

FIG. 1. Polarization of right-hand $\vec{E}^+$, $\vec{H}^+$ (a) and left-hand $\vec{E}^-$, $\vec{H}^-$ (b) waves in chiral isotropic medium. Both waves propagate to the observer (along positive z'-axis direction).

the phase velocity of these waves in a common way, i.e.,

$$V_{\mathrm{ph}\pm} = \frac{\omega}{k_\pm} = \frac{c}{n_\pm}, \tag{21}$$

then $V_{\mathrm{ph}+} < V_{\mathrm{ph}-}$ if $n_\pm > 0$.

Naturally, all the above formulas are also valid for an isotropic nonchiral medium (for example, vacuum), where $\varkappa = 0$ and $n_+ = n_- = n = \sqrt{\varepsilon\mu}$. In the case of an interface between a vacuum and a chiral medium (Sec. III), it is convenient to describe the field in the vacuum area using potentials (8) in both media.

III. GENERAL SOLUTION OF THE PROBLEM

The geometry of the problem is shown in Fig. 2. We will investigate the radiation of a point charge q flying from a standard nonchiral medium ($z < 0$) into a chiral isotropic medium ($z > 0$) described with the use of relations (1). In short, we will identify the area $z < 0$ as a vacuum area; however, we assume only that $\varkappa_v = 0$ while maintaining permittivity $\varepsilon_v \neq 1$ and permeability $\mu_v \neq 1$ (consequently, $n_{v\pm} = n_v = \sqrt{\varepsilon_v\mu_v}$). All values in the vacuum area will have index v, while values in the chiral medium will have the index m. We also introduce the corresponding cylindrical frame r, φ, z. The charge moves with constant velocity $\vec{V}$ along the z axis, such that its position at the moment t is $x = y = r = 0$, $z = Vt$, and therefore

$$\rho = q\delta(x)\delta(y)\delta(z - Vt), \quad \vec{j} = \vec{e}_z V\rho, \tag{22}$$

$$\rho_\omega = \frac{q}{(2\pi)^2 V}\exp\left(\frac{i\omega z}{V}\right)\int_0^\infty J_0(rk_r)k_r dk_r,$$
$$j_\omega = V\rho_\omega. \tag{23}$$

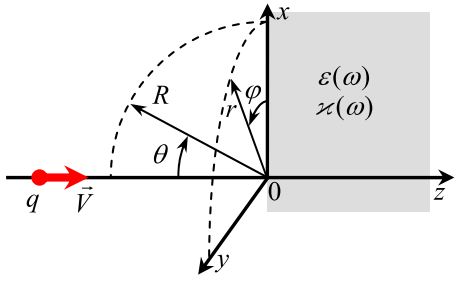

FIG. 2. Geometry of the problem and main notations.

We present a total field in the form

$$\vec{E}_\omega = \vec{E}^q_\omega + \vec{E}^b_\omega, \quad \vec{H}_\omega = \vec{H}^q_\omega + \vec{H}^b_\omega, \tag{24}$$

where $\vec{E}^q_\omega$, $\vec{H}^q_\omega$ is a self-field of the charge in corresponding infinite medium [particular solution of inhomogeneous equations (9)], while $\vec{E}^b_\omega$, $\vec{H}^b_\omega$ is an additional field describing the influence of the boundary [solution of homogeneous equations (9)] [24,37–40]. It is convenient to introduce potentials (8) in each half-space:

$$\vec{E}^{q,bv}_\omega = \vec{E}^{q,bv+}_\omega + \vec{E}^{q,bv-}_\omega,$$
$$\vec{H}^{q,bv}_\omega = i\frac{n_v}{\mu_v}\left(\vec{E}^{q,bv+}_\omega - \vec{E}^{q,bv-}_\omega\right), \tag{25}$$
$$\vec{E}^{q,bm}_\omega = \vec{E}^{q,bm+}_\omega + \vec{E}^{q,bm-}_\omega,$$
$$\vec{H}^{q,bm}_\omega = i\frac{n_m}{\mu_m}\left(\vec{E}^{q,bm+}_\omega - \vec{E}^{q,bm-}_\omega\right), \tag{26}$$

and present them as inverse Fourier-Bessel integrals over the radial wave vector k_r. As follows from the results of the paper [21], the longitudinal potentials of the self-field in chiral medium are

$$E^{qm\pm}_{\omega z} = \frac{iq}{2\pi\omega}\frac{\mu_m s^2_{m\pm}}{n_{m\pm}n_m}\exp\left(i\frac{\omega}{V}z\right)\int_0^{+\infty} dk_r \frac{k_r J_0(k_r r)}{k_r^2 - s^2_{m\pm}}, \tag{27}$$

where $s^2_{m\pm} = \omega^2 V^{-2}(n^2_{m\pm}\beta^2 - 1)$, $n_{m\pm} = n_m \pm \varkappa_m$, $n_m = \sqrt{\varepsilon_m\mu_m}$, $\beta = V/c$. The longitudinal potentials of the self-field in vacuum can be written in the form

$$E^{qv\pm}_{\omega z} = \frac{iq}{2\pi\omega}\frac{\mu_v s^2_v}{n^2_v}\exp\left(i\frac{\omega}{V}z\right)\int_0^{+\infty} dk_r \frac{k_r J_0(k_r r)}{k_r^2 - s^2_v}, \tag{28}$$

where $s^2_v = \omega^2 V^{-2}(n^2_v\beta^2 - 1)$. An additional field is presented in the following form:

$$E^{bv\pm}_{\omega z} = \frac{iq}{2\pi\omega}\int_0^{+\infty} dk_r\, B^v_\pm(k_r)k_r J_0(k_r r)\exp\left(ik^v_z|z|\right), \tag{29}$$

$$E^{bm\pm}_{\omega z} = \frac{iq}{2\pi\omega}\int_0^{+\infty} dk_r\, B^m_\pm(k_r)k_r J_0(k_r r)\exp\left(ik^{m\pm}_z|z|\right), \tag{30}$$

where $B^{v,m}_\pm(k_r)$ are the functions to be found, and the longitudinal wave vectors are

$$k^v_z = \sqrt{\omega^2 c^{-2} n^2_v - k^2_r}, \quad \mathrm{Im}\, k^v_z > 0, \tag{31}$$

$$k^{m\pm}_z = \sqrt{\omega^2 c^{-2} n^2_{m\pm} - k^2_r}, \quad \mathrm{Im}\, k^{m\pm}_z > 0. \tag{32}$$

Usually, radicals are fixed by the conditions $\mathrm{Im}\, k^{v,m\pm}_z > 0$ because corresponding waves should decay away from the interface if we consider nonzero dissipation (the case of nondissipative medium can be considered as a result of the corresponding limiting process). One can show that the following properties hold (overline denotes complex conjugate):

$$k^v_z(-\bar{\omega}) = -\overline{k^v_z(\omega)}, \quad k^{m\pm}_z(-\bar{\omega}) = -\overline{k^{m\mp}_z(\omega)}. \tag{33}$$

Using boundary conditions in the plane $z = 0$, one can derive coefficients $B^{v,m}_\pm(k_r)$, which determine the longitudinal field, (29) and (30), and calculate transversal components with the use of formulas presented in Appendix A (see Appendix B).

After that, the additional field in vacuum area can be divided into two groups:

$$\begin{Bmatrix} E^{bv}_{\omega\rho} \\ E^{bv}_{\omega z} \\ H^{bv}_{\omega\varphi} \end{Bmatrix} = \frac{iq}{2\pi\omega}\int_0^{+\infty} dk_r \begin{Bmatrix} ik_z^v J_1(k_r r) \\ k_r J_0(k_r r) \\ -i\omega c^{-1}\varepsilon_v J_1(k_r r) \end{Bmatrix} B^v_{\mathrm{co}} \exp\left(ik_z^v|z|\right), \tag{34}$$

$$\begin{Bmatrix} H^{bv}_{\omega\rho} \\ H^{bv}_{\omega z} \\ E^{bv}_{\omega\varphi} \end{Bmatrix} = \frac{iq}{2\pi\omega}\int_0^{+\infty} dk_r \begin{Bmatrix} -n_v\mu_v^{-1}k_z^v J_1(k_r r) \\ in_v\mu_v^{-1}k_r J_0(k_r r) \\ -\omega c^{-1} n_v J_1(k_r r) \end{Bmatrix} B^v_{\mathrm{cr}} \exp\left(ik_z^v|z|\right), \tag{35}$$

where B^v_{co} and B^v_{cr} are determined by (B11) and (B12). Formula (34) describes the field with polarization coinciding with the polarization of the self-field of a moving charge (28) and (B14), and therefore we will refer to this field as copolarization. In contrast, the field described by formula (35) will be referred to as cross-polarization.

In the case of weak chirality,

$$|\tilde{\varkappa}| \ll 1, \quad \tilde{\varkappa} = \varkappa_m n_m^{-1}, \tag{36}$$

one can perform the following decompositions (up to first-order terms with respect to $\tilde{\varkappa}$):

$$n_{m\pm} = n_m(1 \pm \tilde{\varkappa}), \tag{37}$$

$$k_z^{m\pm} \approx k_z^m\left[1 \pm \frac{k_m^2\tilde{\varkappa}}{\left(k_z^m\right)^2}\right], \quad k_m^2 = \frac{\omega^2}{c^2}n_m^2,$$

$$k_z^m = \sqrt{\frac{\omega^2}{c^2}n_m^2 - k_r^2}, \quad \operatorname{Im} k_z^m > 0, \tag{38}$$

$$s_{m\pm}^2 \approx s_m^2\left(1 \pm \frac{2n_m^2\omega^2\tilde{\varkappa}}{s_m^2 c^2}\right), \quad s_m^2 = \frac{\omega^2}{V^2}\left(n_2^2\beta^2 - 1\right), \tag{39}$$

$$\Delta_c \approx \Delta_0 = n_m\left(\varepsilon_v k_z^v + \varepsilon_m k_z^m\right)\left(\frac{k_z^v}{\mu_v} + \frac{k_z^m}{\mu_m}\right). \tag{40}$$

We obtain

$$B^v_{\mathrm{co}} \underset{|\tilde{\varkappa}|\ll 1}{\approx} \frac{2k_r^2}{\left(\varepsilon_v k_z^v + \varepsilon_m k_z^m\right)} \times\left[\frac{\omega V^{-1}\varepsilon_m\varepsilon_v^{-1} - k_z^m}{k_r^2 - s_v^2} - \frac{1}{\omega V^{-1} + k_z^m}\right], \tag{41}$$

$$B^v_{\mathrm{cr}} \underset{|\tilde{\varkappa}|\ll 1}{\approx} \frac{2k_r^2\tilde{\varkappa}}{n_v\Delta_0}\left(\frac{n_m^2 k_z^m\left[1 - k_m^2\left(k_z^m\right)^{-2}\right]}{\mu_m\left(\omega V^{-1} - k_z^v\right)} + \frac{1}{\omega V^{-1} + k_z^m}\left\{\frac{\varepsilon_v k_m^2}{k_z^m}\left(1 + \frac{k_z^m}{\omega V^{-1} + k_z^m}\right) + \frac{k_z^v n_m^2}{\mu_m}\left[1 + \frac{k_m^2\left(k_z^m\right)^{-2}}{\omega V^{-1} + k_z^m}\right]\right\}\right). \tag{42}$$

The copolarization coefficient (41) does not depend on chirality in the first-order approximation and coincides with the corresponding expression for a nonchiral medium [24]. The cross-polarization coefficient (42) is proportional to $\varkappa_m$, and therefore the cross-polarized wave can be observed in the linear approximation. In the case $\varkappa_m = 0$, cross-polarization is absent, and the expressions for the field components coincide perfectly with the known results for a nonchiral medium [24,37–40]. Thus, the presence of the cross-polarization wave in the vacuum area is a distinctive feature of an interface with a chiral medium.

IV. RADIATION IN THE VACUUM AREA

Here, asymptotic analysis of the additional field (34) and (35) in the vacuum area is performed. Using a standard procedure, in these expressions, we can transform semi-infinite integrals to infinite ones that contain Hankel functions $H_0^{(1)}(k_r r)$ instead of Bessel functions. We introduce a spherical coordinate system R, θ, φ as shown in Fig. 2. Note that angle θ is counted off from the negative direction of the z axis, and therefore the unit vectors $\vec{e}_R$, $\vec{e}_\varphi$, $\vec{e}_\theta$ form a right-hand orthogonal set, and

$$r = R\sin\theta, \quad z = -R\cos\theta. \tag{43}$$

We also introduce new integration variable ψ as follows:

$$k_r = k_v\sin\psi, \quad k_z^v = k_v\cos\psi, \quad k_v = k_0 n_v. \tag{44}$$

Then, the longitudinal components (transversal components can be handled similarly) can be written in the form

$$\begin{Bmatrix} E^{bv}_{\omega z} \\ H^{bv}_{\omega z} \end{Bmatrix} = \frac{iqk_v^2}{8\pi\omega}\int_{\Gamma_\psi} \sin 2\psi\, H_0^{(1)}(\Omega\sin\theta\sin\psi) \times \begin{Bmatrix} B^v_{\mathrm{co}}(k_v\sin\psi) \\ \dfrac{in_v}{\mu_v}B^v_{\mathrm{cr}}(k_v\sin\psi) \end{Bmatrix} \exp\left(i\Omega\cos\psi\cos\theta\right)d\psi, \tag{45}$$

where $\Omega = Rk_v$ and Γ_ψ is an integration path in the complex plane ψ. In the far-field zone determined by the condition $|\Omega| \gg 1$, the asymptotic analysis of integrals (45) can be performed by the use of saddle-point method [41]. Using the asymptotic of the Hankel function for $|\Omega\sin\theta\sin\psi| \gg 1$ [42], we obtain

$$\begin{Bmatrix} E^{bv}_{\omega z} \\ H^{bv}_{\omega z} \end{Bmatrix} = \frac{iqk_v^2}{8\pi\omega}\int_{\Gamma_\psi} \sin 2\psi\sqrt{\frac{2}{\pi\Omega\sin\theta\sin\psi}} \times e^{\frac{-i\pi}{4}} \begin{Bmatrix} B^v_{\mathrm{co}}(k_v\sin\psi) \\ \dfrac{in_v}{\mu_v}B^v_{\mathrm{cr}}(k_v\sin\psi) \end{Bmatrix} \exp\left(\Omega\varphi_v\right)d\psi, \tag{46}$$

where

$$\varphi_v = i\cos\left(\psi - \theta\right). \tag{47}$$

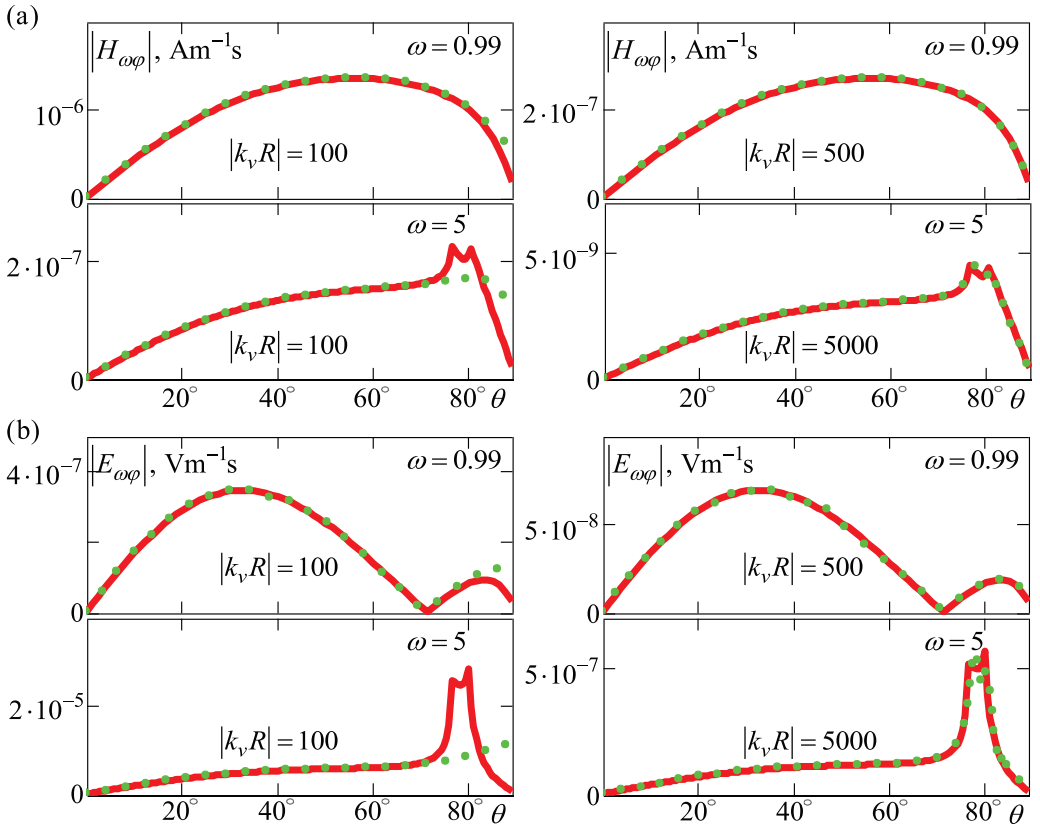

FIG. 3. Angular dependencies of copolarization component $H_{\omega\varphi}$ (a) and cross-polarization component $E_{\omega\varphi}$ (b) over angle θ for $q = -1$ nC, $\beta = 0.6$ and for two values of frequency (in units of $\omega_{\rm rm}$) in the case of the Condon model (61) with the following parameters: $\omega_{\rm rm} = \omega_{\rm pm} = 2\pi \times 10$ GHz, $\omega_0 = 0.03\omega_{\rm pm}$, $\omega_{\rm dm} = 10^{-3}\omega_{\rm pm}$, $\omega_{\rm pv} = 10^{-4}\omega_{\rm pm}$, $\omega_{\rm dv} = 10^{-3}\omega_{\rm pv}$. The green points correspond to the calculation via rigorous integral formulas (34) and (35), and the red solid line corresponds to the calculation via asymptotic formulas (54) and (55).

The saddle point is $\psi_s = \theta$, and the corresponding steepest descent path (SDP) $\Gamma_{\rm SDP}$ can be calculated. Then, we should transform Γ_ψ to $\Gamma_{\rm SDP}$. The integral over SDP is determined mainly by the contribution of the saddle point (since $|\Omega| \gg 1$). In this case, we obtain the contribution of the saddle point as follows:

$$\begin{Bmatrix} E^{bv}_{\omega z} \\ H^{bv}_{\omega z} \end{Bmatrix} \approx \begin{Bmatrix} E^{v\rm rad}_{\omega z} \\ H^{v\rm rad}_{\omega z} \end{Bmatrix} = \frac{qk_v \cos\theta}{2\pi\omega} \begin{Bmatrix} B^v_{\rm co}(k_v \sin\theta) \\ \dfrac{in_v}{\mu_v} B^v_{\rm cr}(k_v \sin\theta) \end{Bmatrix} \frac{\exp(ik_v R)}{R}. \quad (48)$$

Note that the integrands in (34) and (35) have singular points, such as poles

$$k_r = \pm s_v, \quad s_v = \sqrt{s_v^2}, \quad \operatorname{Im} s_v > 0, \quad (49)$$

$$k_r = \pm s^{\pm}_m, \quad s_{m\pm} = \sqrt{s^2_{m\pm}}, \quad \operatorname{Im} s_{m\pm} > 0, \quad (50)$$

and branch points

$$k_r = \pm\sqrt{k_0^2 n_v^2}, \quad k_r = \pm\sqrt{k_0^2 n^2_{m\pm}}, \quad \operatorname{Im}\sqrt{\ } > 0. \quad (51)$$

The integrands in (45) also have corresponding poles and branch points, excluding the branch points $k_r = \pm\sqrt{k_0^2 n_v^2}$, which are eliminated by substitution (44). It can be shown that the poles do not contribute to (46). For certain parameters, the transformation $\Gamma_\psi \to \Gamma_{\rm SDP}$ is accompanied by the capture of branch points, and corresponding contributions to the field are connected by the generation of so-called lateral waves [43]. Thus, Eq. (48), which does not consider such contributions, is not valid for the mentioned parameters. However, in Sec. V, we will calculate the field numerically using exact integral representations (34) and (35) and show that the lateral waves can be neglected for sufficiently large distances.

Calculating the transversal components of the field and rewriting them in spherical coordinates, we obtain for copolarization $E^{v\rm rad}_{\omega R} = 0$,

$$\begin{Bmatrix} E^{v\rm rad}_{\omega\theta} \\ H^{v\rm rad}_{\omega\varphi} \end{Bmatrix} = \frac{q\cot\theta}{2\pi\omega} B^v_{\rm co}(k_v \sin\theta) \begin{Bmatrix} k_v \\ -\omega\varepsilon_v \\ \hline c \end{Bmatrix} \frac{\exp(ik_v R)}{R}, \quad (52)$$

and for cross-polarization $H^{v\rm rad}_{\omega R} = 0$,

$$\begin{Bmatrix} H^{v\rm rad}_{\omega\theta} \\ E^{v\rm rad}_{\omega\varphi} \end{Bmatrix} = \frac{iqn_v \cot\theta}{2\pi\omega} B^v_{\rm cr}(k_v \sin\theta) \begin{Bmatrix} k_v \\ \mu_v \\ k_0 \end{Bmatrix} \frac{\exp(ik_v R)}{R}, \quad (53)$$

These formulas describe the volume radiation in the far-field zone defined by the inequality $k_v R \gg 1$ (for real positive k_v). There are two transversal spherical waves with linear polarization. They have identical phase velocity, and the vectors of the electric fields of these waves are mutually orthogonal. If

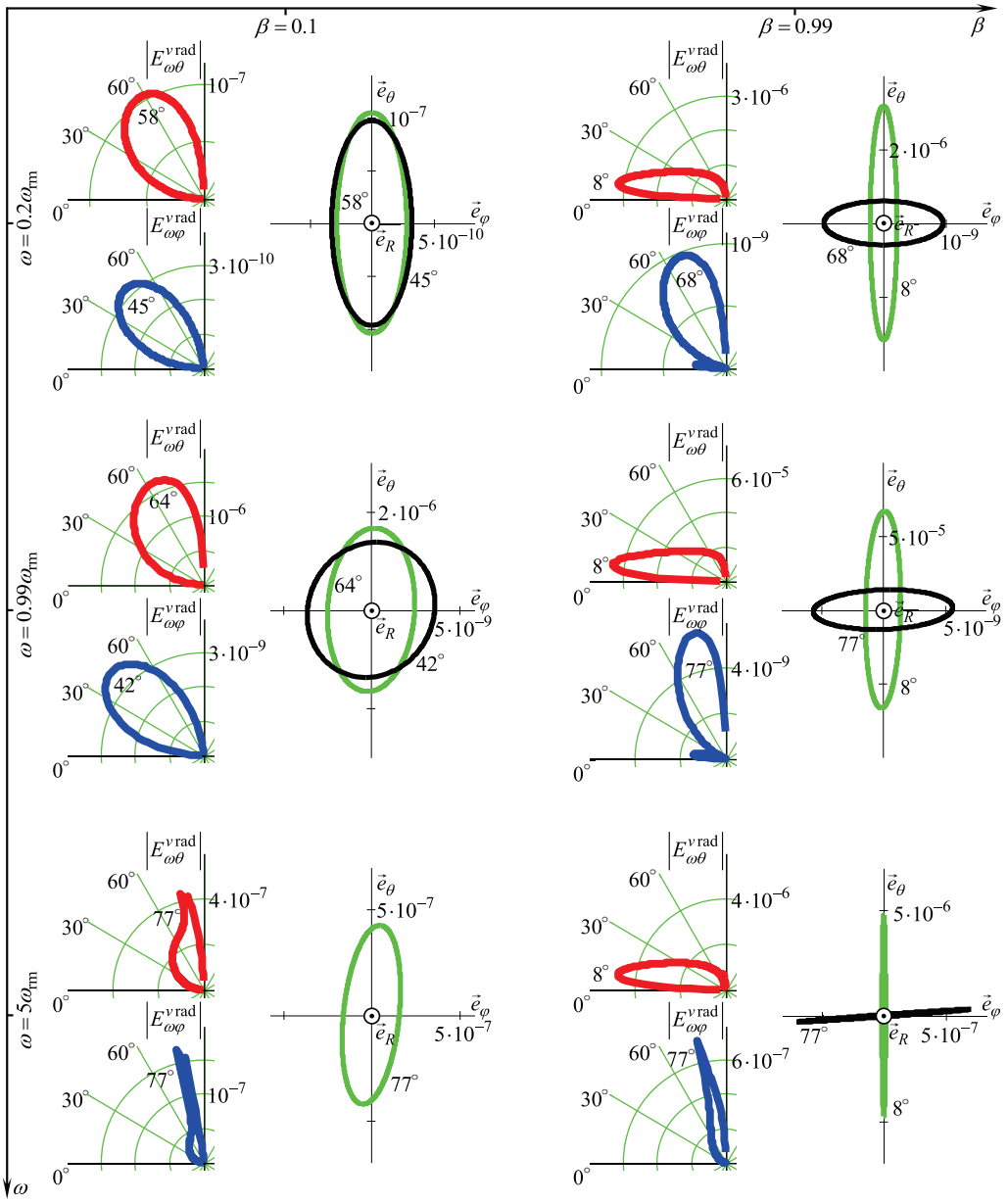

FIG. 4. Radiation patterns ($E^{v\mathrm{rad}}_{\omega}$ is in $\mathrm{Vm}^{-1}\,\mathrm{s}$) and ellipses of polarization (calculated for a lobe maximum) for $q = -1\,\mathrm{nC}$ and various charge velocities β and frequencies ω of the Condon model (61) with relatively weak chirality (chiral parameter $\omega_0 = 0.03\omega_{\mathrm{pm}}$). Other media parameters are as follows: $\omega_{\mathrm{rm}} = \omega_{\mathrm{pm}} = 2\pi\times 10\,\mathrm{GHz}$, $\omega_{\mathrm{dm}} = 10^{-3}\omega_{\mathrm{pm}}$, $\omega_{\mathrm{pv}} = 10^{-4}\omega_{\mathrm{pm}}$, $\omega_{\mathrm{dv}} = 10^{-3}\omega_{\mathrm{pv}}$.

we set $\varepsilon_v = \mu_v = 1$, then $n_v = 1$, and therefore

$$E^{v\mathrm{rad}}_{\omega\theta} = -H^{v\mathrm{rad}}_{\omega\varphi} = \frac{q\cot\theta}{2\pi c} B^{v}_{\mathrm{co}}(k_0\sin\theta)\frac{\exp(ik_0R)}{R}, \quad (54)$$

$$H^{v\mathrm{rad}}_{\omega\theta} = E^{v\mathrm{rad}}_{\omega\varphi} = \frac{iq\cot\theta}{2\pi c} B^{v}_{\mathrm{cr}}(k_0\sin\theta)\frac{\exp(ik_0R)}{R}. \quad (55)$$

If dissipation in a chiral medium is negligible and coefficients B^{v}_{co} and B^{v}_{cr} are purely real, then the phase difference between the waves (54) and (55) is equal to $\pi/2$, and the summary wave in vacuum is characterized by elliptic polarization with the main axes $\vec{e}_\theta$ and $\vec{e}_\varphi$. In other cases, the polarization ellipse is rotated over some angle depending on the phase of the polarization coefficient

$$P = |P|e^{i\varphi_P} = \frac{E^{v\mathrm{rad}}_{\omega\varphi}}{E^{v\mathrm{rad}}_{\omega\theta}} = i\left.\frac{B^{v}_{\mathrm{cr}}}{B^{v}_{\mathrm{co}}}\right|_{k_r=k_0\sin\theta}. \quad (56)$$

Let us calculate the ellipses of polarization. In the harmonic regime, we have in the far-field zone:

$$\begin{aligned}\vec{E}^{v\mathrm{rad}}(t) &= 2\,\mathrm{Re}\left[\vec{E}^{v\mathrm{rad}}_{\omega}\exp(-i\omega t)\right]\\ &= \frac{q\cot\theta}{\pi Rc}\left|B^{v}_{\mathrm{co}}(k_0\sin\theta)\right|\left\{\vec{e}_\theta\cos\left[\omega\left(\frac{R}{c}-t\right)+\varphi_{\mathrm{co}}\right]\right.\\ &\quad\left.+\vec{e}_\varphi|P|\sin\left[\omega\left(\frac{R}{c}-t\right)+\varphi_{\mathrm{co}}+\varphi_P\right]\right\}\\ &= \vec{e}_\theta E_\theta(t)+\vec{e}_\varphi E_\varphi(t), \end{aligned} \quad (57)$$

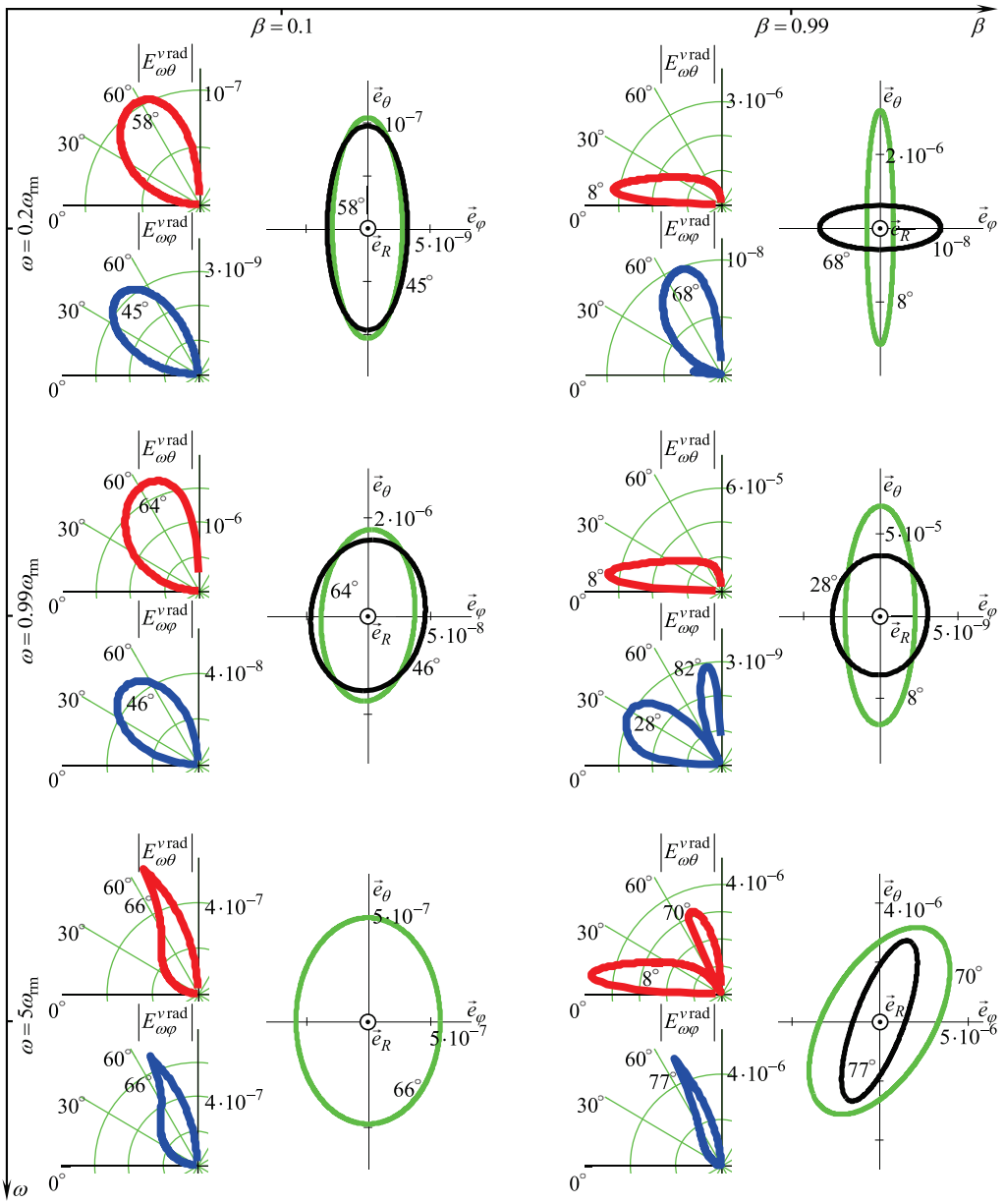

FIG. 5. Radiation patterns ($E^{v\mathrm{rad}}_{\omega}$ is in $\mathrm{Vm}^{-1}\,\mathrm{s}$) and ellipses of polarization (calculated for a lobe maximum) for $q = -1\,\mathrm{nC}$ and various charge velocities β and frequencies ω of the Condon model (61) with relatively strong chirality (chiral parameter $\omega_0 = 0.3\omega_{\mathrm{pm}}$ is 10 times larger compared with that in Fig. 4). Other medium parameters are the same.

where φ_{co} is the phase of $B^{v}_{\mathrm{co}}(k_0 \sin\theta)$. If $(Rc^{-1} - t)$ increases and the wave propagates to the observer, vector $\vec{E}$ rotates counterclockwise in the plane orthogonal to $\vec{e}_R$.

Excluding time dependence from (57), we can obtain the following relation:

$$\frac{E_\varphi^2}{E_0^2|P|^2} + \frac{E_\theta^2}{E_0^2} - 2\frac{E_\varphi E_\theta}{E_0^2|P|}\cos\varphi_P = (\sin\varphi_P)^2, \tag{58}$$

where

$$E_0 = \frac{qk_0}{\pi\omega}\frac{\cot\theta}{R}\left|B^{v}_{\mathrm{co}}(k_0\sin\theta)\right|. \tag{59}$$

Equation (58) determines the polarization ellipse, i.e., the hodograph of the vector $\vec{E}^{v\mathrm{rad}}(t)$. As one can deduce from (58), the main axes of this ellipse are rotated with respect to $\vec{e}_\theta$ and $\vec{e}_\varphi$ at the angle ψ_{pe} determined by the following relation:

$$\tan 2\psi_{\mathrm{pe}} = 2|P|\cos\varphi_P(|P|^2 - 1)^{-1}. \tag{60}$$

Angle ψ_{pe} differs from zero if φ_P differs from $\pi/2$. The polarization ellipses will be calculated in Sec. V.

V. NUMERICAL RESULTS

The frequency dependencies of $\varepsilon_m(\omega)$ and $\varkappa_m(\omega)$ in accordance with Condon dispersion model [3] are determined by the following relations:

$$\varepsilon_m(\omega) = 1 + \omega_{\mathrm{pm}}^2\left[\omega_{\mathrm{rm}}^2 - 2i\omega\omega_{\mathrm{dm}} - \omega^2\right]^{-1},$$
$$\varkappa_m(\omega) = \omega_0\omega\left[\omega_{\mathrm{rm}}^2 - 2i\omega_{\mathrm{dm}}\omega - \omega^2\right]^{-1}, \tag{61}$$

where $\omega_{\rm rm}$ is a medium resonant frequency, $\omega_{\rm pm}$ is an analog of plasma frequency, $\omega_{\rm dm}$ is a parameter responsible for dissipation, and ω_0 is a chiral parameter. Further, to illustrate the main effects, we will calculate the Fourier harmonics and related values for two or three typical frequencies of the model (61). For a vacuum area, we will use a cold plasma model with dissipation

$$\varepsilon_v(\omega) = 1 - \omega_{\rm pv}^2[2i\omega_{\rm dv}\omega + \omega^2]^{-1}, \tag{62}$$

under the assumption that $\omega_{\rm pv} \ll \omega_{\rm pm}$. In this case, $\varepsilon_v \approx 1$ for all frequencies of interest, while model (62) is a convenient way to introduce losses correctly.

First, we should clarify the statement concerning the applicability of the saddle-point approximation (48). Figure 3 compares the angular dependencies calculated using asymptotic formulas (54) and (55) [these formulas follow from (48)] and rigorous integral formulas (34) and (35). Since the integrands in (34) and (35) are quickly oscillating functions, the convergence of calculations is achieved by dividing the essential area of integration into the appropriate number of subareas. For large distances, such calculation takes essential time.

In Fig. 3, angle $\theta = 0^\circ$ corresponds to the trajectory of the charge motion, while $\theta = 90^\circ$ corresponds to the boundary (see Fig. 2). The component $H_{\omega\varphi}$ determines the field with copolarization, while the component $E_{\omega\varphi}$ determines the field with cross-polarization. As shown by Fig. 3, for a relatively small distance ($|k_v R| = 100$, left column), the two curves coincide throughout essentially the whole range of angles, excluding some in the vicinity of the boundary. For angles θ close to 90°, branch points contribute to the integrals (46), which means that lateral waves are generated near the boundary. Rigorously speaking, the asymptotic formulas (54) and (55) are not valid for these angles and this R. However, with increasing distance R, the relative contribution of the lateral waves becomes smaller compared with the contribution of the spherical waves of the transition radiation (Fig. 3, right column). For example, for $\omega = 0.99$, the distance $R = 500|k_v|^{-1}$ is large enough for the difference between curves become invisible. For $\omega = 5$, lateral waves become insignificant for distances $R \geqslant 5000|k_v|^{-1}$ because angular dependencies practically coincide for this R. We can conclude that the angular distribution of the field components is described correctly by asymptotic representations (54) and (55) for sufficiently large distance R. Such distances will be referred to henceforth as the far-field zone.

Figure 4 shows the radiation patterns in the far-field zone for two frequencies of the Condon model with relatively weak chirality ($\omega_0 = 0.03\omega_{\rm pm}$) calculated using (54) and (55) for relatively small ($\beta = 0.1$) and relatively large ($\beta = 0.99$) charge velocity. In most cases, the radiation patterns have a single lobe. For $\omega = 0.99\omega_{\rm rm}$, the lobe for the $E_{\omega\theta}^{\rm vrad}$ component is usually several orders of magnitude larger than the lobe for $E_{\omega\varphi}^{\rm vrad}$. Thus, the cross-polarized wave is excited weakly. However, for large frequency ($\omega = 5\omega_{\rm rm}$), these lobes are of the same order of magnitude, and therefore co- and cross-polarized waves are comparable. Figure 4 also shows ellipses of polarization calculated for the angles of the lobe maxima (angles indicated near each lobe). It is supposed that the corresponding wave propagates to the observer (along $\vec{e}_R$). In most cases, these ellipses are strongly prolonged along the $\vec{e}_\theta$ direction. However, for $\omega = 5\omega_{\rm rm}$ and $\beta = 0.1$, the polarization ellipse has relatively weak prolongation.

Figure 5 illustrates the radiation patterns and ellipses of polarization for relatively strong chirality ($\omega_0 = 0.3\omega_{\rm pm}$ is ten times larger than in Fig. 4, and other media parameters are the same). The essential difference with Fig. 4 occurs for relativistic charge velocity ($\beta = 0.99$), where the radiation patterns have two lobes. Polarization ellipses have relatively weak prolongation for $\omega = 5\omega_{\rm rm}$, that is, co- and cross-polarized waves are comparable (for $\beta = 0.1$ the ellipse is close to circle). In addition, for $\beta = 0.99$, these ellipses have their axes rotated by a considerable angle.

VI. CONCLUSION

In this paper, we have investigated the radiation produced by a point charge flying from a vacuum into a chiral isotropic medium described by the Condon dispersion model. This medium itself supports two fundamental transversal electromagnetic waves with right-hand and left-hand circular polarizations. We have deduced the analytical expression describing the field generated by point charge in both vacuum and medium. The distinguishing feature of this field in the vacuum area is that it contains two waves with different polarizations, one coinciding with the polarization of the self-field of the charge (copolarization), while the other is orthogonal to the polarization of the charge's self-field (cross-polarization). Since these two waves are coherent (have the same propagation velocity), they form a total wave with elliptical polarization.

By applying saddle-point approximation to rigorous integral representations of the field components, we have calculated the field in the far-field zone. This field is a sum of two transversal spherical waves of transition radiation, one with copolarization and the other with cross-polarization. Based on these asymptotic formulas, we have calculated the radiation patterns and ellipses of polarizations for the case of interface between the vacuum and Condon chiral medium for various frequencies (in the harmonic regime) and charge velocities. We have shown that in most cases, the radiation patterns for both the copolarized and cross-polarized field have a single main lobe, but the angles of maxima can differ significantly. The lobe for cross-polarization is typically several orders of magnitude smaller than for copolarization, and therefore the corresponding ellipses of polarization are strongly prolonged. However, for relatively large frequency (several resonant frequencies of the chiral medium), these magnitudes can be comparable, and therefore the corresponding ellipses can be close to a circle (that is, the co- and cross-polarized waves are comparable). For relatively strong chirality and relativistic charge velocity, the radiation patterns can have two lobes with comparable magnitudes.

ACKNOWLEDGMENT

This work is supported by the Grant of the Russian Foundation for Basic Research (No. 15-32-20985).

APPENDIX A: CONNECTION BETWEEN LONGITUDINAL AND TRANSVERSAL COMPONENTS OF THE FIELD

For analysis performed in Sec. III, it is convenient to obtain some expressions connecting "longitudinal" and "transversal" components of the field. We introduce another Cartesian frame x, y, z determined by the direction of the external current: it is supposed that $\vec{j}_\omega = j_\omega \vec{e}_z$. The direction along the z axis will be called "longitudinal," while directions orthogonal to the z axis will be called "transversal." Decomposing the field

$$\vec{E}_\omega = \vec{E}_{\omega\perp} + E_{\omega z}\vec{e}_z, \quad \vec{E}_{\omega\perp} = E_{\omega x}\vec{e}_x + E_{\omega y}\vec{e}_y, \tag{A1}$$

one can obtain from (6)

$$\begin{aligned}
\Delta_\perp \vec{E}^+_{\omega\perp} &= \frac{2\pi}{n_+}\frac{\mu}{\sqrt{\varepsilon\mu}}\nabla_\perp\rho_\omega + \frac{2\pi}{c}\frac{i\mu}{\sqrt{\varepsilon\mu}}\mathrm{rot}(\vec{e}_z j_\omega) - \frac{1}{2}\nabla_\perp\frac{\partial E^+_{\omega z}}{\partial z} + \frac{k_0}{2}n_+\mathrm{rot}(\vec{e}_z E^+_{\omega z}),\\
\Delta_\perp \vec{E}^-_{\omega\perp} &= \frac{2\pi}{n_-}\frac{\mu}{\sqrt{\varepsilon\mu}}\nabla_\perp\rho_\omega - \frac{2\pi}{c}\frac{i\mu}{\sqrt{\varepsilon\mu}}\mathrm{rot}(\vec{e}_z j_\omega) - \frac{1}{2}\nabla_\perp\frac{\partial E^-_{\omega z}}{\partial z} - \frac{k_0}{2}n_-\mathrm{rot}(\vec{e}_z E^-_{\omega z}),
\end{aligned} \tag{A2}$$

where

$$\Delta_\perp \vec{E}_{\omega\perp} = \vec{e}_x\Delta_\perp E_{\omega x} + \vec{e}_y\Delta_\perp E_{\omega y}, \quad \Delta_\perp E_{\omega x,y} = \frac{\partial^2 E_{\omega x,y}}{\partial x^2} + \frac{\partial^2 E_{\omega x,y}}{\partial y^2}, \quad \nabla_\perp = \vec{e}_x\frac{\partial}{\partial x} + \vec{e}_y\frac{\partial}{\partial y}. \tag{A3}$$

Equation (A2) gives the relation between the longitudinal and transversal components of potentials $\vec{E}^\pm_\omega$. In cylindrical coordinates r, φ, z, for the case where dependence on φ is absent (cylindrical symmetry is supposed), one obtains from (A2) the equations

$$\frac{\partial^2 E^\pm_{\omega r}}{\partial r^2} + \frac{1}{r}\frac{\partial E^\pm_{\omega r}}{\partial r} - \frac{1}{r^2}E^\pm_{\omega r} = \frac{2\pi}{n_\pm}\frac{\mu}{\sqrt{\varepsilon\mu}}\frac{\partial\rho_\omega}{\partial r} - \frac{1}{2}\frac{\partial^2 E^\pm_{\omega z}}{\partial r\partial z}, \quad \frac{\partial^2 E^\pm_{\omega\varphi}}{\partial r^2} + \frac{1}{r}\frac{\partial E^\pm_{\omega\varphi}}{\partial r} - \frac{1}{r^2}E^\pm_{\omega\varphi} = \mp\frac{1}{2}\frac{\omega n_\pm}{c}\frac{\partial E^\pm_{\omega z}}{\partial r} \mp \frac{2\pi}{c}\frac{i\mu}{\sqrt{\varepsilon\mu}}\frac{\partial j_{\omega z}}{\partial r}. \tag{A4}$$

These expressions are used in Appendix B.

APPENDIX B: SOLUTION OF THE BOUNDARY VALUE PROBLEM

In the plane $z = 0$, due to the boundary conditions, the r and φ components of the total field should be continuous:

$$\left\{\begin{matrix} E^{v+}_{\omega r} + E^{v-}_{\omega r} \\ E^{v+}_{\omega\varphi} + E^{v-}_{\omega\varphi}\end{matrix}\right\}\Bigg|_{z=-0} = \left\{\begin{matrix} E^{m+}_{\omega r} + E^{m-}_{\omega r} \\ E^{m+}_{\omega\varphi} + E^{m-}_{\omega\varphi}\end{matrix}\right\}\Bigg|_{z=+0}, \quad \frac{n_v}{\mu_v}\left\{\begin{matrix} E^{v+}_{\omega r} - E^{v-}_{\omega r} \\ E^{v+}_{\omega\varphi} - E^{v-}_{\omega\varphi}\end{matrix}\right\}\Bigg|_{z=-0} = \frac{n_m}{\mu_m}\left\{\begin{matrix} E^{m+}_{\omega r} - E^{m-}_{\omega r} \\ E^{m+}_{\omega\varphi} - E^{m-}_{\omega\varphi}\end{matrix}\right\}\Bigg|_{z=+0}. \tag{B1}$$

Using relations (A4), we can rewrite these conditions for the longitudinal components of the potentials:

$$\frac{8\pi\mu_v}{n_v^2}\rho_\omega - \left(\frac{\partial E^{v+}_{\omega z}}{\partial z} + \frac{\partial E^{v-}_{\omega z}}{\partial z}\right)\Bigg|_{z=0} = \frac{4\pi\mu_m}{n_m}\frac{n_{m+}+n_{m-}}{n_{m+}n_{m-}}\rho_\omega - \left(\frac{\partial E^{m+}_{\omega z}}{\partial z} + \frac{\partial E^{m-}_{\omega z}}{\partial z}\right)\Bigg|_{z=0}, \tag{B2}$$

$$n_v E^{v+}_{\omega z} - n_v E^{v-}_{\omega z}\big|_{z=0} = n_{m+}E^{m+}_{\omega z} - n_{m-}E^{m-}_{\omega z}\big|_{z=0}, \tag{B3}$$

$$-\frac{n_v}{\mu_v}\left(\frac{\partial E^{v+}_{\omega z}}{\partial z} - \frac{\partial E^{v-}_{\omega z}}{\partial z}\right)\Bigg|_{z=0} = 4\pi\frac{n_{m-}-n_{m+}}{n_{m+}n_{m-}}\rho_\omega - \frac{n_m}{\mu_m}\left(\frac{\partial E^{m+}_{\omega z}}{\partial z} - \frac{\partial E^{m-}_{\omega z}}{\partial z}\right)\Bigg|_{z=0}, \tag{B4}$$

$$\frac{n_v}{\mu_v}\left(n_v E^{v+}_{\omega z} + n_v E^{v-}_{\omega z}\right)\big|_{z=0} = \frac{n_m}{\mu_m}\left(n_{m+}E^{m+}_{\omega z} + n_{m-}E^{m-}_{\omega z}\right)\big|_{z=0}. \tag{B5}$$

After a series of transformations, we obtain from (B2)–(B5) the following system of equations for the unknown functions $B^v_\pm$, $B^m_\pm$:

$$\begin{aligned}
\frac{-qk^v_z}{\pi\omega}(B^v_+ + B^v_-) - \frac{qk^{m+}_z}{\pi\omega}B^m_+ - \frac{qk^{m-}_z}{\pi\omega}B^m_- &= -\frac{2q}{\pi V\varepsilon_v} - \frac{2q}{\pi V\varepsilon_v}\frac{s_v^2}{k_r^2 - s_v^2} + \frac{q\mu_m}{\pi V n_m}\frac{n_{m+}+n_{m-}}{n_{m+}n_{m-}}\\
&\quad + \frac{q\mu_m}{\pi V n_m}\left(\frac{1}{n_{m+}}\frac{s^2_{m+}}{k_r^2 - s^2_{m+}} + \frac{1}{n_{m-}}\frac{s^2_{m-}}{k_r^2 - s^2_{m-}}\right),
\end{aligned} \tag{B6}$$

$$\frac{iqn_v}{\pi\omega}(B^v_+ - B^v_-) - \frac{iqn_{m+}}{\pi\omega}B^m_+ - \frac{iqn_{m-}}{\pi\omega}B^m_- = \frac{iq\mu_m}{\pi\omega n_m}\left(\frac{s^2_{m+}}{k_r^2 - s^2_{m+}} - \frac{s^2_{m-}}{k_r^2 - s^2_{m-}}\right), \tag{B7}$$

$$\frac{-qk_z^v}{\pi\omega}\frac{n_v}{\mu_v}(B_+^v - B_-^v) - \frac{qn_m}{\pi\omega\mu_m}\left(k_z^{m+}B_+^m - k_z^{m-}B_-^m\right) = \frac{q}{\pi V}\frac{n_{m-}-n_{m+}}{n_{m+}n_{m-}} + \frac{q}{\pi V}\left(\frac{1}{n_{m+}}\frac{s_{m+}^2}{k_r^2-s_{m+}^2} - \frac{1}{n_{m-}}\frac{s_{m-}^2}{k_r^2-s_{m-}^2}\right), \tag{B8}$$

$$\frac{iq\varepsilon_v}{\pi\omega}(B_+^v + B_-^v) - \frac{iqn_m}{\pi\omega\mu_m}(n_{m+}B_+^m + n_{m-}B_-^m) = \frac{-2iq}{\pi\omega}\frac{s_v^2}{k_r^2 - s_v^2} + \frac{iq}{\pi\omega}\left(\frac{s_{m+}^2}{k_r^2 - s_{m+}^2} + \frac{s_{m-}^2}{k_r^2 - s_{m-}^2}\right). \tag{B9}$$

It is convenient to rewrite these equations with respect to new functions:

$$B_{\mathrm{co}}^v(k_r) = B_+^v(k_r) + B_-^v(k_r), \quad B_{\mathrm{cr}}^v(k_r) = B_+^v(k_r) - B_-^v(k_r). \tag{B10}$$

After a large amount of algebraic calculations, we obtain

$$B_{\mathrm{co}}^v(k_r) = \frac{k_r^2}{\Delta_c}\frac{\left(\frac{k_z^v n_{m-}}{\mu_v} + \frac{n_m}{\mu_m}k_z^{m-}\right)\left(\frac{\omega}{V}\frac{\varepsilon_m}{\varepsilon_v}\frac{n_{m+}}{n_m} - k_z^{m+}\right)}{k_r^2 - s_v^2} + \frac{k_r^2}{\Delta_c}\frac{\left(\frac{k_z^v n_{m+}}{\mu_v} + \frac{n_m}{\mu_m}k_z^{m+}\right)\left(\frac{\omega}{V}\frac{\varepsilon_m}{\varepsilon_v}\frac{n_{m-}}{n_m} - k_z^{m-}\right)}{k_r^2 - s_v^2}$$
$$- \frac{k_r^2}{\Delta_c}\left(\frac{\frac{k_z^v n_{m-}}{\mu_v} + \frac{n_m}{\mu_m}k_z^{m-}}{\omega V^{-1} + k_z^{m+}} + \frac{\frac{k_z^v n_{m+}}{\mu_v} + \frac{n_m}{\mu_m}k_z^{m+}}{\omega V^{-1} + k_z^{m-}}\right), \tag{B11}$$

$$B_{\mathrm{cr}}^v(k_r) = \frac{k_r^2}{\Delta_c}\frac{1}{n_v}\left[\frac{n_m}{\mu_m}\frac{\left(n_{m+}k_z^{m-} - n_{m-}k_z^{m+}\right)}{\omega V^{-1} + k_z^v} - \frac{\varepsilon_v k_z^{m-} + n_m\mu_m^{-1}n_{m-}k_z^v}{\omega V^{-1} + k_z^{m+}} + \frac{\varepsilon_v k_z^{m+} + n_m\mu_m^{-1}n_{m+}k_z^v}{\omega V^{-1} + k_z^{m-}}\right], \tag{B12}$$

$$\Delta_c = \frac{n_m}{2\mu_m}\left[n_{m+}\left(\frac{k_z^v n_{m-}}{\mu_v} + \frac{n_m}{\mu_m}k_z^{m-}\right)\left(\frac{k_z^{m+}\varepsilon_v\mu_m}{n_{m+}n_m} + k_z^v\right) + n_{m-}\left(\frac{k_z^v n_{m+}}{\mu_v} + \frac{n_m}{\mu_m}k_z^{m+}\right)\left(\frac{k_z^{m-}\varepsilon_v\mu_m}{n_{m-}n_m} + k_z^v\right)\right], \tag{B13}$$

where Δ_c is a determinant of the system (B6)–(B9). For the sake of brevity, we do not present here the cumbersome expressions for $B_\pm^m$ because we will further investigate the field in the vacuum area only.

The transversal components of the self-field in the vacuum area are known [21]:

$$\begin{Bmatrix} E_{\omega r}^{qv\pm} \\ E_{\omega\varphi}^{qv\pm} \end{Bmatrix} = \frac{q}{2\pi}\frac{\mu_v}{n_v}\begin{Bmatrix} (Vn_v)^{-1} \\ (ic)^{-1} \end{Bmatrix}\exp\left(i\frac{\omega}{V}z\right)\int_0^{+\infty} dk_r \frac{k_r^2 J_1(k_r r)}{k_r^2 - s_v^2}. \tag{B14}$$

The transversal components of the additional field are

$$\begin{Bmatrix} E_{\omega\rho}^{bv\pm} \\ E_{\omega\varphi}^{bv\pm} \end{Bmatrix} = \frac{iq}{2\pi\omega}\int_0^{+\infty} dk_r \begin{Bmatrix} C_\pm^v(k_r) \\ D_\pm^v(k_r) \end{Bmatrix} k_r J_0(k_r r)\exp\left(ik_z^v|z|\right). \tag{B15}$$

Coefficients $C_\pm^v$, $D_\pm^v$ can be found from (A2):

$$C_\pm^v = \frac{ik_z^v}{k_r}B_\pm^v, \quad D_\pm^v = \mp k_0\frac{n_v}{k_r}B_\pm^v. \tag{B16}$$

Therefore, the field in the vacuum area is fully determined.

[1] B. Kahr and O. Arteaga, Chem. Phys. Chem. **13**, 79 (2012).
[2] F. I. Fedorov, *Theory of Gyrotropy* (Nauka i technika, Minsk, 1976).
[3] I. V. Lindell, A. H. Sihvola, S. A. Tretyakov, and A. J. Viitanen, *Electromagnetic Waves in Chiral and Bi-isotropic Media* (Artech House, Boston, London, 1994).
[4] E. U. Condon, Rev. Mod. Phys. **9**, 432 (1937).
[5] S. A. Tretyakov, Radiotekhnika i Elektronika **39**, 1457 (1994).
[6] J. Lekner, Pure Appl. Opt. **5**, 417 (1996).
[7] P. Fischer and F. Hache, Chirality **17**, 421 (2005).
[8] D. G. Blackmond, Cold Spring Harb. Perspect. Biol. **2**, a002147 (2010).
[9] R. P. Cameron and S. M. Barnett, Phys. Chem. Chem. Phys. **16**, 25819 (2014).
[10] P. A. Čerenkov, Phys. Rev. **52**, 378 (1937).
[11] I. E. Tamm and I. M. Frank, Compt. Rend. Acad. Sci. USSR **14**, 109 (1937).
[12] B. M. Bolotovskii, Phys. Usp. **62**, 201 (1957).
[13] J. V. Jelley, *Čerenkov Radiation and Its Applications* (Pergamon Press, New York, 1958).
[14] V. P. Zrelov, *Vavilov-Cherenkov Radiation in High-Energy Physics* (Israel Program for Scientific Translations, Jerusalem, 1970).
[15] A. A. Kolomenskii, Zh. Eksp. Teor. Fiz. **24**, 167 (1953).
[16] V. A. Belyakov, Nucl. Instr. Meth. Phys. Res. A **248**, 20 (1986).
[17] N. Engheta and S. Bassiri, J. Appl. Phys. **68**, 4393 (1990).
[18] A. Lakhtakia, Optik **87**, 133 (1991).
[19] K. A. Barsukov and A. A. Smirnova, Tech. Phys. **44**, 328 (1999).
[20] P. Hillion, Turk. J. Phys. **30**, 115 (2006).
[21] S. N. Galyamin, A. A. Peshkov, and A. V. Tyukhtin, Phys. Rev. E **88**, 013206 (2013).
[22] M. Schäferling, D. Dregely, M. Hentschel, and H. Giessen, Phys. Rev. X **2**, 031010 (2012).

[23] S. N. Galyamin, D. Y. Kapshtan, and A. V. Tyukhtin, Phys. Rev. E **87**, 013109 (2013).
[24] V. L. Ginzburg and V. N. Tsytovich, *Transition Radiation and Transition Scattering* (Hilger, London, 1990).
[25] N. Engheta and A. Mickelson, IEEE Trans. Antennas Propag. **30**, 1213 (1982).
[26] C. Li, G. S. Mitchell, and S. R. Cherry, Opt. Lett. **35**, 1109 (2010).
[27] Z. Hu, J. Liang, W. Yang, W. Fan, C. Li, X. Ma, X. Chen, X. Ma, X. Li, X. Qu, J. Wang, F. Cao, and J. Tian, Opt. Express **18**, 24441 (2010).
[28] A. E. Spinelli, F. Boschi, D. D'Ambrosio, L. Calderan, M. Marengo, A. Fenzi, M. Menegazzi, A. Sbarbati, A. Del Vecchio, and R. Calandrino, Nucl. Instr. Meth. Phys. Res. A **648**, S310 (2011).
[29] A. E. Spinelli and F. Boschi, J. Biomed. Opt. **16**, 120507 (2011).
[30] J. Zhong, C. Qin, X. Yang, S. Zhu, X. Zhang, and J. Tian, Int. J. Biomed. Imaging **2011**, 641618 (2011).
[31] D. L. J. Thorek, R. Robertson, W. A. Bacchus, J. Hahn, J. Rothberg, B. J. Beattie, and J. Grimm, Am. J. Nucl. Med. Mol. Imaging **2**, 163 (2012).
[32] A. D. Klose, Y. Tekabe, and L. Johnson, in *Biomedical Optics 2014* (Optical Society of America, Miami, FL, 2014), p. BW3B.3.
[33] H. Liu, X. Yang, T. Song, C. Bao, L. Shi, Z. Hu, K. Wang, and J. Tiana, J. Biomed. Opt. **20**, 086007 (2015).
[34] M. Mathew, Cerenkov photons: A cancer searchlight (unpublished).
[35] A. E. Spinelli, M. Ferdeghini, C. Cavedon, E. Zivelonghi, R. Calandrino, A. Fenzi, A. Sbarbati, and F. Boschi, J. Biomed. Opt. **18**, 020502 (2013).
[36] A. S. Sihvola and I. V. Lindell, Microwave Opt. Tech. Lett. **4**, 295 (1991).
[37] S. N. Galyamin, A. V. Tyukhtin, A. Kanareykin, and P. Schoessow, Phys. Rev. Lett. **103**, 194802 (2009).
[38] S. N. Galyamin and A. V. Tyukhtin, Phys. Rev. B **81**, 235134 (2010).
[39] S. N. Galyamin and A. V. Tyukhtin, Phys. Rev. E **84**, 056608 (2011).
[40] T. Y. Alekhina and A. V. Tyukhtin, Phys. Rev. E **83**, 066401 (2011).
[41] L. B. Felsen and N. Marcuvitz, *Radiation and Scattering of Waves* (Wiley Interscience, Hoboken, NJ, 2003).
[42] H. Bateman and A. Erdelyi, *Higher Transcendental Functions* (McGraw-Hill, New York, 1953).
[43] L. M. Brekhovskih, *Waves in Layered Media* (Academic Press, New York, 1980).